GA–A24870

COMPARISON OF BROAD SPECTRUM TURBULENCE MEASUREMENTS AND GYROKINETIC CODE PREDICTIONS ON THE DIII–D TOKAMAK

by
T.L. RHODES, W.A. PEEBLES, M. van ZEELAND, D. MIKKELSEN,
M.A. GILMORE, X.V. NGUYEN, D.R. BAKER, J.C. DeBOO,
J.S. deGRASSIE, W. DORLAND, E.J. DOYLE,
C.M. GREENFIELD, C.C. PETTY, and L. ZENG

NOVEMBER 2004

GENERAL ATOMICS

DISCLAIMER

GA–A24870

COMPARISON OF BROAD SPECTRUM TURBULENCE MEASUREMENTS AND GYROKINETIC CODE PREDICTIONS ON THE DIII–D TOKAMAK

by
T.L. RHODES,* W.A. PEEBLES,* M. van ZEELAND, D. MIKKELSEN,[†]
M.A. GILMORE,[‡] X.V. NGUYEN,* D.R. BAKER, J.C. DeBOO,
J.S. deGRASSIE, W. DORLAND,[◊] E.J. DOYLE,*
C.M. GREENFIELD, C.C. PETTY, and L. ZENG

*University of California, Los Angeles, California, USA
[†]Princeton Plasma Physics Laboratory, Princeton, New Jersey, USA
[‡]University of New Mexico, Albuquerque, New Mexico, USA
[◊]University of Maryland, College Park, Maryland, USA

This is a preprint of a paper to be presented at the 20th IAEA Fusion Energy Conference, Vilamoura, Portugal, November 1–6, 2004 and to be printed in the Proceedings.

Work supported by
the U.S. Department of Energy
under DE-FC02-04ER54698, DE-FG03-01ER54615,
DE-AC02-76CH03073, SC-6832401
and DE-FG02-93ER54197

GENERAL ATOMICS PROJECT 30200
NOVEMBER 2004

GENERAL ATOMICS

Comparison of Broad Spectrum Turbulence Measurements and Gyrokinetic Code Predictions on the DIII-D Tokamak

T.L. Rhodes,[1] W.A. Peebles,[1] M. Van Zeeland,[2] D. Mikkelsen,[3] M.A. Gilmore,[4] X.V. Nguyen,[1] D.R. Baker,[2] J.C. DeBoo,[2] J.S. deGrassie,[2] W. Dorland,[5] E.J. Doyle,[1] C.M. Greenfield,[2] C.C. Petty,[2] and L. Zeng[1]

[1]University of California, Los Angeles, California, USA
email: Rhodes@fusion.gat.com
[2]General Atomics, P.O. Box 85608, San Diego, California 92186-5608, USA
[3]Princeton Plasma Physics Laboratory, Princeton, New Jersey, USA
[4]University of New Mexico, Albuquerque, New Mexico, USA
[5]University of Maryland, College Park, Maryland, USA

Abstract. Density fluctuation measurements over a broad wavenumber range (low-k, 0–2 cm^{-1}, intermediate-k, 8–15 cm^{-1}, and high-k, ~35 cm^{-1}) have recently been performed for the first time on DIII-D which provide a new, more complete picture of turbulence behavior in a tokamak. This wavenumber range corresponds to $k_\perp\rho_s \approx 0.2 \rightarrow 10$, a range relevant to ITG, TEM and ETG type instabilities. Calculations using the GKS linear instability code indicated the plasma was indeed unstable to ITG, TEM, and ETG and therefore consistent with the observed turbulent activity. Additionally, qualitative agreement between the predicted frequency ranges and measurements were found. Detailed plasma instabilities tests were performed by separately using short duration neutral beam blips and electron cyclotron heating to modify the plasma parameters. These perturbations modified the background temperature and density as well as the density fluctuation behavior. It was found that both the measured and calculated response to these perturbations varied with wavenumber, supporting the need for broad wavenumber comparisons. The measured fluctuation changes and predicted growth rates results showed both similarities and differences. These observations could be due to complex interactions not contained in the linear code and are under investigation using more complete non-linear turbulence simulations.

1. Introduction

The understanding of anomalous electron and ion transport leading to development of a predictive transport capability represents a significant experimental and theoretical challenge. It is generally acknowledged that long wavelength turbulence in the form of ion temperature gradient (ITG: $k_\perp\rho_s \sim 0.1$) driven modes is likely responsible for anomalous ion transport. Anomalous electron thermal transport is often theoretically attributed to shorter scale, trapped electron (TEM: $k_\perp\rho_s \sim 1$) or electron temperature gradient (ETG: $k_\perp\rho_s \sim 10$) driven turbulence, which are little affected by ExB shear suppression. Furthermore, the interaction of these instabilities may prove crucial to improved understanding. Progress will result in improved confidence in extrapolation to next-step fusion devices and, potentially, lead to improved transport control and enhanced fusion performance. Detailed comparison of transport properties and broad wavenumber range turbulence measurements to theoretical predictions is essential in developing this predictive capability. Due to the possible interaction of these various wavenumber ranges and the possibility of their differing response to plasma conditions it is important to make these measurements simultaneously or near simultaneously.

A broad wavenumber diagnostic set is being developed at DIII-D to address anomalous electron and ion transport. The UCLA FIR scattering system has been upgraded to probe low (0–2 cm^{-1}) and intermediate wavenumbers (8–15 cm^{-1}) and a new concept high-k backscattering system has been added for high-k (~ 35 cm^{-1}). The U. Wisc. beam emission spectroscopy system (BES) was recently upgraded for improved sensitivity and probes 0–3.5 cm^{-1} while fluctuation and correlation reflectometry probe 0–5 cm^{-1}. The MIT phase contrast imaging system (PCI) has been upgraded to probe the core plasma with wavenumbers in the range, 0-8 cm^{-1} and 20-100 cm^{-1}. Shown in Fig. 1 is a schematic representation of the diagnostic wavenumber range covered along with the relevant instability wavenumbers. The diagnostic k space is large and covers much of the relevant wavenumbers.

In this paper are presented experimental measurements of density fluctuations over a broad wavenumber range (0–35 cm^{-1}). The focus will be on the FIR scattering system and mm-wave backscattering system. Later reports will expand these results to include the other available diagnostics. An outline of the paper is as follows. First a brief overview of the fluctuation diagnostics used is given, followed by initial measurements and comparisons to linear growth rate calculations from the GKS code [1]. These initial measurements are found to be qualitatively consistent with the linear GKS calculations. A discussion of these findings is then presented. Following this are data from experiments which modify the theoretical growth rates using neutral beam injection and electron cyclotron heating. Here the goal was to deliberately modify the plasma parameters so as to change the predicted growth rates. Comparisons between these calculated growth rates and the measured fluctuation levels are then made and discussed. It is found that there is some agreement with predicted changes but also some interesting differences.

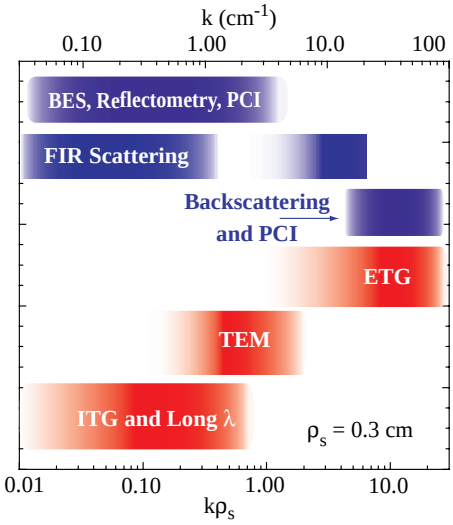

Fig. 1. Diagram showing wavenumber and $k\rho_s$ space comparing diagnostic wavenumber ranges on DIII-D with representative plasma instability wavenumbers.

2. Low and Intermediate Wavenumber Measurements Using FIR Scattering

A far infrared (FIR) forward scattering system operating at 288 GHz was used to monitor density fluctuations in the range 0–2 cm^{-1} and 8–15 cm^{-1}. The split wavenumber range covers the low-k part of the turbulent spectrum where much of the turbulent power is thought to reside while the intermediate k range (8–15 cm^{-1}) covers the transition region between the trapped electron mode and electron temperature gradient modes. The system utilizes solid state sources, quasi-optical beam focusing elements, and flat and parabolic metal mirrors. Forward scattering at small angles (±1°) probes long wavelength turbulence (k~0–2 cm^{-1}) while also allowing for interferometric phase measurement. Forward scattering at larger angles (8–15°) probes larger wavenumber fluctuations (k~8-15 cm^{-1}). The wavenumbers detected are dominantely poloidal wavenumbers. The system has a wavenumber resolution of approximately ±1 cm^{-1} and a frequency response to more than 10 MHz for the low-k and 45 MHz for the intermediate-k. The FIR probe beam is oriented radially along the tokamak midplane.The low-k channel samples a chord average along this beam while the intermediate-k channel is more spatially localized depending upon the wavenumber chosen.

A primary concern in such a system is that the relatively large amplitude, low-k signals do not contaminate the low amplitude, intermediate-k signals. Very good separation between the low and intermediate-k signals was found in both the laboratory and with plasmas. The low-k and intermediate-k signals had quite different qualitative behavior, i.e. Doppler broadening, differences in response to L-to-H transitions, pellets, etc. For example, during neutral beam injection the low-k signal has a much smaller Doppler broadening than the intermediate-k consistent with their different wavenumbers. The coherency between the low and intermediate-k signals was found to be near zero (the coherency is a frequency resolved measure of the linear correlation between the two channels and the small value indicates extremely low to no cross-contamination of one signal by the other) indicating that the two channels were observing different wavenumbers. It was also important to verify that the signal from the intermediate-k channel was due to plasma fluctuations at the desired wavenumber. A test of this was to vary the intermediate-k wavenumber while viewing a fixed radial position. This should result in a variation of the Doppler shifted frequency, $\Delta\omega = \mathbf{k} \cdot \mathbf{V}$,

which is proportional to the wavenumber chosen, where **V** is the local E×B poloidal velocity. It was found that the ratio of the Doppler broadening of the signals is approximately the same (within about 10%) as the ratio of wavenumbers indicating that the intermediate-k channel was detecting the correct wavenumber.

3. High Wavenumber Measurements Using mm-Wave Back Scattering

A mm-wave backscatter approach was used to monitor high-k (30–40 cm^{-1}) fluctuations. The physics of the measurement method is the same as the FIR forward scattering described above with the exception that the observation angle is very near 180° with respect to the probe beam (whereas the FIR scattering angle is 0–15°). A high power (200 mW) 94 GHz solid state source was employed together with standard waveguide receiver and coupling components. Figure 2 shows the integration of the mm-wave backscatter and FIR low-k systems. The 94 GHz incident and backscattered radiation are shown as a single solid red line in Fig. 2. Only a single line occurs because in this 180° backscatter geometry the scattered radiation retraces the incident radiation path. Also in the figure the solid blue line corresponds to the FIR 288 GHz incident and scattered radiation. As indicated in Fig. 2, the $2f_{ce}$ resonance acts as an internal "beam dump" absorbing both the incident and forward scattered radiation from low k turbulence. The exact location of this beam dump can be varied by changing the toroidal magnetic field strength. The back scattered radiation retraces the propagation path of the input radiation and is detected. Any unwanted O-mode radiation that is launched strikes the inner wall at an angle and is not reflected back to the receiver. The signal from the mm-wave backscatter diagnostic then comes from a chord which starts at the plasma edge and ends at the electron cyclotron resonance location. Finally, it should be noted that backscatter observes principally radial k while the FIR scattering is principally poloidal k.

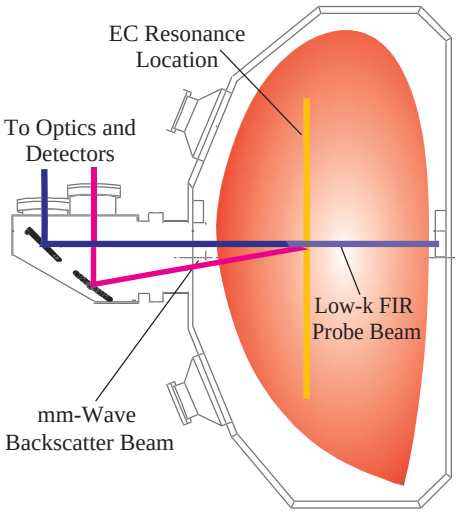

Fig. 2. Diagram illustrating the diagnostic geometry for the low-k FIR forward scattering and the high-k mm-wave backscattering systems. The electron cyclotron resonance location is shown.

Multiple tests of the mm-wave backscattering were performed. The backscatter signal was clearly different from the lower-k signals, for example showing none of the coherent modes often seen at low-k. No coherency was found between the low-k FIR and backscattered signal. Interestingly, the concept of wavenumber matching provided an excellent test of the system performance. In scattering theory, if the wavenumber being probed does not physically align in such a way as to satisfy the momentum balance then no scattering occurs. More detailed calculations show that wavenumber matching can occur for non-zero mismatch angles (Eq. 11 in [2]). Backscattering measurements were made with different incident angles which tested this prediction. The results of this angular scan agreed well with the theoretical instrument response confirming the operation of the diagnostic.

4. Initial Measurement Results and Comparison to Linear Instability Predictions (GKS code)

Utilizing these new DIII-D diagnostic capabilities, initial measurements of low (0–1 cm^{-1}), intermediate (15 cm^{-1}), and high-k (40 cm^{-1}) density fluctuations relevant to the ITG, TEM, and ETG wavenumber ranges were made. These data were acquired in an Ohmic, diverted plasma, I_p = 1 MA, $n_{e,avg} = 2.6\times10^{19}$ m^{-3}, B_T = 2.1 T. High-k (~40 cm^{-1}) data from the new backscattering system show broadband fluctuation activity out to ~1 MHz [Fig. 3(a)].

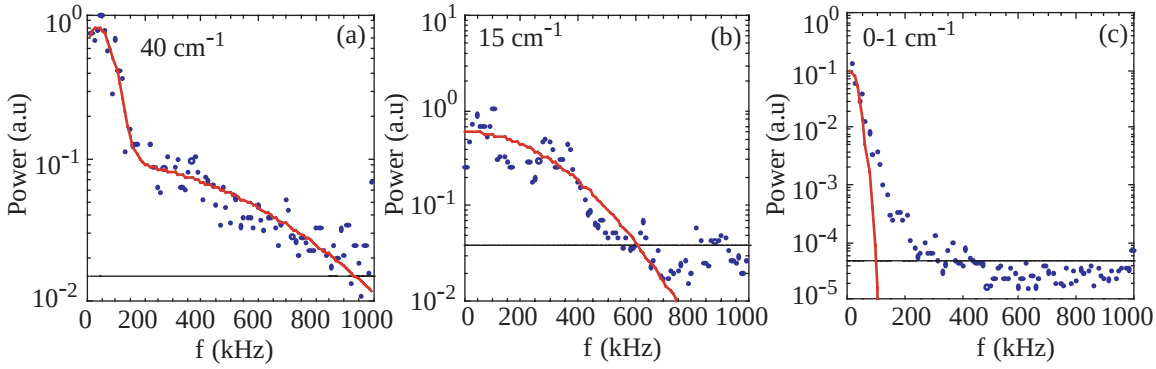

Fig. 3. Frequency spectra from: (a) backscattering diagnostic, radial-k dominant, $k_r \sim 40$ cm^{-1}. (b) intermediate-k FIR scattering, $k_\theta = 15$ cm^{-1}, and (c) low-k FIR scattering, $k_\theta = 0$-1 cm^{-1}. Red lines are Gaussian fits to the data while the noise floor is indicated by horizontal lines.

Intermediate-k data (~15 cm^{-1}), from the upgraded FIR scattering system, is less broadband than the 40 cm^{-1} data, with the k range consistent with ETG/TEM [Fig. 3(b)]. Low-k (0-1 cm^{-1}) FIR [Fig. 3(c)] and reflectometry (0-5 cm^{-1}) data are in an ITG wavenumber range with spectra more narrow still. Shown in Fig. 3 are Gaussian fits to the data as well as noise floors. The high-k data are well fit by two Gaussians, one relatively narrow with a width of ~50 kHz, and the other broad with a width ~490 kHz. The Gaussian widths of the 15 and 0-1 cm^{-1} data are 260 kHz and 24 kHz respectively. Not shown are spectra from reflectometer systems showing frequency widths of 20–70 kHz. The observed trend is for increasing frequency width with increasing wavenumber. The relatively narrow, low frequency (f < 200 kHz) peak in the high-k data [Fig. 3(a)] is different in spectral shape and time behavior from the broader part of the high-k spectrum. This interesting observation may be due to a spatial variation of the turbulence intensity and is under investigation, experimentally and theoretically.

Calculations using the GKS linear stability code indicate that these discharges are unstable to a wide range of instabilities: ETG, ITG and TEM. Figure 4 shows the predicted real frequency of the unstable modes over the radial range r = 0.1–0.9 for different k values. Note that negative real frequencies indicate propagation in the ion diamagnetic direction, consistent with ITG features, while positive frequencies are consistent with electron type modes, e.g. TEM and/or ETG. Figure 4 indicates that the frequency range predicted at 40 cm^{-1} is larger than that at 15 cm^{-1} which is in turn larger than the 1 cm^{-1} prediction. The predicted frequencies are somewhat smaller than those seen experimentally but are nevertheless in qualitative agreement with the measured spectra [Fig. 3(a-c)]. The GKS calculations of the frequency are only an approximate indication of how the fully developed turbulence would behave, but they do provide a guide as to how the instabilities might appear. In addition, while the GKS code calculates poloidal wavenumber characteristics, the high-k data (40 cm^{-1}) are principally radial k. If the fluctuations are isotropic in k_r-k_θ then the simulation and experiment are directly comparable. However, if there is a significant anisotropy, for example due to streamer activity, then nonlinear simulations are needed to estimate the expected frequency range of the backscattered signal. Nonlinear simulations

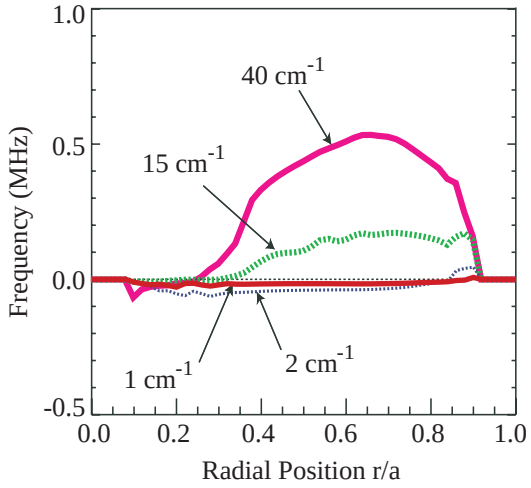

Fig. 4. GKS predictions of real frequency for 1, 2, 15 and 40 cm^{-1} for the plasma conditions of Fig. 3.

(GS2) are underway which will both address this issue as well as extend the experiment-simulation comparisons.

5. Testing Theoretical Predictions Using Perturbation Techniques: Comparison of Experimental Measurements and Linear Instability Calculations

Linear growth rates of the various plasma instabilities are predicted to vary with the local variables, T_e, T_i, L_n, L_T, Z_{eff}, etc. Theoretically, the ratio of electron to ion temperature T_e/T_i, density and temperature scale lengths, L_n, L_T, and impurity concentration are expected to affect the growth rates of the low and high k fluctuations in different ways (e.g. see [3–5]). For example, increasing T_e/T_i is believed to increase the ITG growth rates while decreasing the ETG growth rates (with all other quantities held fixed). Decreasing L_n (while keeping L_{Te} either constant or increasing it) can theoretically turn off the ETG modes. The experiments described below were designed to modify one or more of these parameters, to measure the fluctuation response over a broad wavenumber range, and to compare these measurements to predictions of various turbulence and instability codes. The measured profiles (n_e, T_e, etc.) are used as code inputs. It is difficult if not impossible to modify one plasma parameter without affecting some or many more. The experimental approach was to attempt to modify only one parameter, but to measure all important ones, and to use these measurements as input into the codes.

5.1. Short Time Duration Neutral Beam Injection

Short time duration neutral beam blips were used to selectively heat the electrons while providing little or no ion heating or density change. Figure 5 shows the neutral beam injection times, response of the electron temperature, and response of low and intermediate-k scattering signals. The neutral beams were injected into a moderately low density Ohmic plasma, with the beam duration increasing from 10 ms, to 20 ms, and finally to 30 ms. The plasma parameters were B_T = 2.1 T, I_p = 0.8 MA, n_{chord} = 2.8×10^{19} m^{-3}. Due to the low electron temperature the beam heating was predominantly on the electrons. A precise measure of the ion heating is difficult to make since the beams are used to determine T_i, however, no consistent change in T_i was found for the beam duration increasing from 10 to 30 ms. The electron temperature response increased with increasing beam duration as seen in Fig. 5(b). Density and electron temperature profiles are shown for the two times indicated by the red and black arrows. The density does not change appreciably while T_e increases across the whole radius [Fig. 5(e) and 5(f)]. The electron temperature increases in time up till the turn off of the beams then decreases. The low and intermediate-k signals, labeled n_{tilde} shown in Fig. 5(c) and 5(d) are RMS levels integrated across the frequency range where the fluctuations appear. These levels are seen to respond quite differently, with the low-k increasing to a maximum after the beam turns off and the intermediate-k decreasing to a minimum. Both signals then return to the pre-beam levels. Not shown are the Doppler broadening of the scattering signals due to the neutral beams. The low

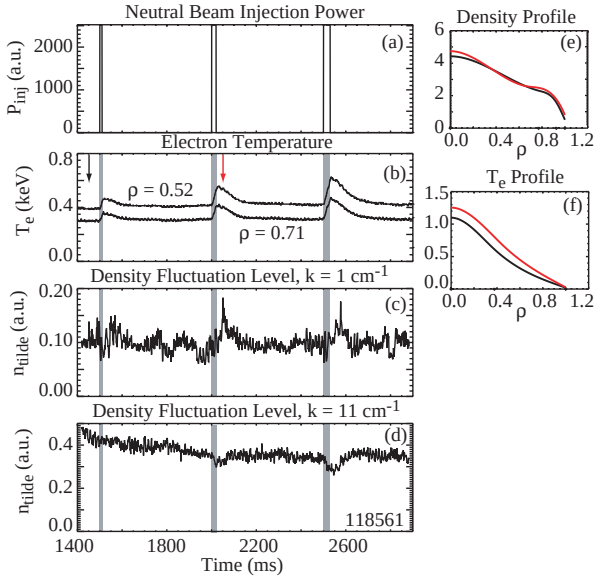

Fig. 5. Time series of (a) neutral beam injection, (b) electron temperature response, (c) integrated fluctuation level for k=1 cm^{-1} from FIR scattering, (d) integrated fluctuation level for k=11 cm^{-1} from FIR scattering, (e) density profiles from two times shown by the arrows in (b), and (f) electron temperature profiles for same two times.

and intermediate k signals see a frequency change of approximately 30 kHz and 400 kHz respectively at the third beam blip. This is an indication that the neutral beam is affecting the plasma rotation and consequently the radial electric field. Figure 6 shows low and high-k data from a different discharge, but with similar beam blips. There the low-k fluctuations increase as they do in Fig. 5(c). Interestingly the high-k fluctuations also increase, in contrast to the response of the intermediate-k shown in Fig. 5(d).

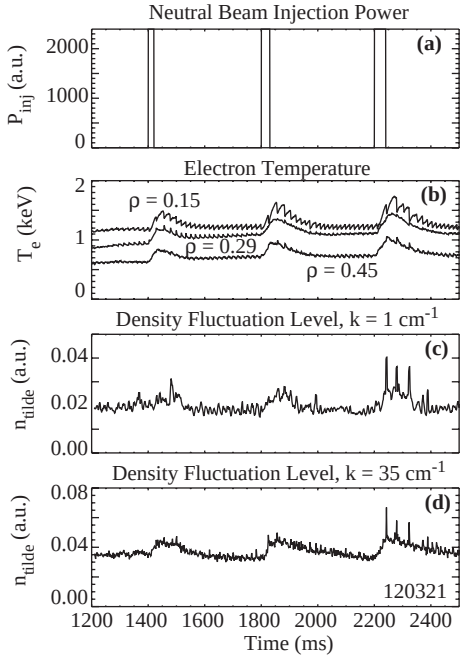

Fig. 6. Time series of (a) neutral beam injection, (b) electron temperature, (c) integrated fluctuation level for k=1 cm^{-1} from FIR scattering, (d) integrated fluctuation level for k=35 cm-1 from mm-wave backscattering from a shot similar to that in Fig. 5.

Linear growth rate calculations using the GKS code were performed for the two times indicated by the arrows in Fig. 5. The major difference in the code inputs was the electron temperature profile. The density, T_i, etc. were essentially identical for the two times. The results of the calculation are shown in Fig. 7 for the three different wavenumbers measured. Plotted are growth rates and real frequency versus radial position. Positive growth rate indicates instability and positive frequency indicates propagation in the electron diamagnetic drift direction. The low-k (k = 1 cm^{-1}) shows an increase in growth rate over much of the radius consistent with the increase flucuation level seen in Fig. 5(c). The real frequency is negative for the majority of the radius indicating a mode propagating in the ion diamagnetic drift direction. Interestingly, the k = 11 cm^{-1} growth rate increases for large radii and decreases for the middle radii. Note that the intermediate-k scattering was centered roughly upon the magnetic axis so that the majority of the signal comes from a radial range centered near $\rho = 0$, with diminishing sensitivity out to $\rho = 1$. Thus the intermediate-k would likely observe any increase in fluctuation levels at the edge, but with reduced response compared to the more central locations. The GKS calculation shows an increase with neutral beams at the edge for the k = 35 cm^{-1} wavenumber. This is qualitatively consistent with the observations shown in Fig. 6 but it should be noted that the calculation was done for the plasma parameters shown in Fig. 5.

5.2. Electron Cyclotron Heating

Electron cyclotron heating (ECH) was applied to a low density, diverted, Ohmic discharge, B_T = 1.9 T, I_p = 0.7 MA, and $n_{chord} = 1.5\times10^{19}$ m^{-3}. Short neutral beam blips of 10 ms duration were applied every 100 ms for diagnostic purposes. The response of the plasma to the ECH was an increase in electron temperature and a slight decrease in density [Fig. 8(b) and 8(c)]. Also shown in Fig. 8(d–f) are the integrated fluctuation signals from low, intermediate and high k. From the figure it is seen that the low-k did not change appreciably with ECH while the intermediate-k decreased somewhat (~10%) and the high-k increased (~10%–15%). The high-k fluctuation level decreases rapidly after ECH turn-off, similar to the T_e signal from the outer part of the plasma [Fig. 8(b)]. It should be noted that T_i did not change appreciably during the ECH.

Linear growth rate calculations were performed for the two times indicated by the arrows in Fig. 8(a) and are shown in Fig. 9 along with the measured fluctuation spectra for the different wavenumbers. For k = 1 cm^{-1} the linear growth rates increase with ECH everywhere

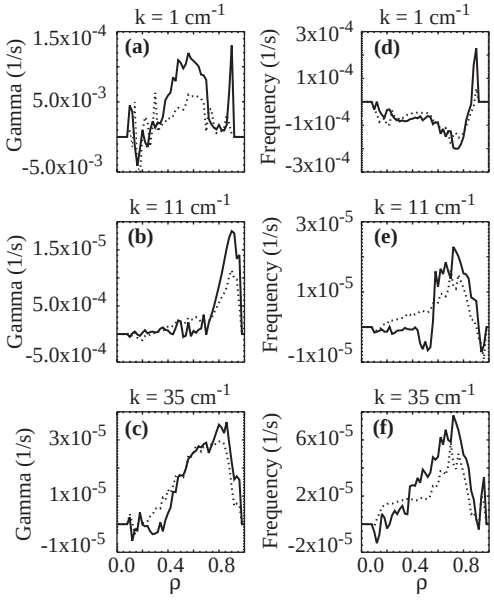

Fig. 7. GKS calculations of linear growth rates versus radial position for plasma shown in Fig. 5. (a) k = 1 cm^{-1}, (b) k = 11 cm^{-1}, (c) k = 35 cm^{-1}. Real frequencies versus radial position for the same wavenumbers are shown in (d)–(f). Dashed line is ohmic phase, 1450 ms, solid line is near peak in T_e response at 2050 ms.

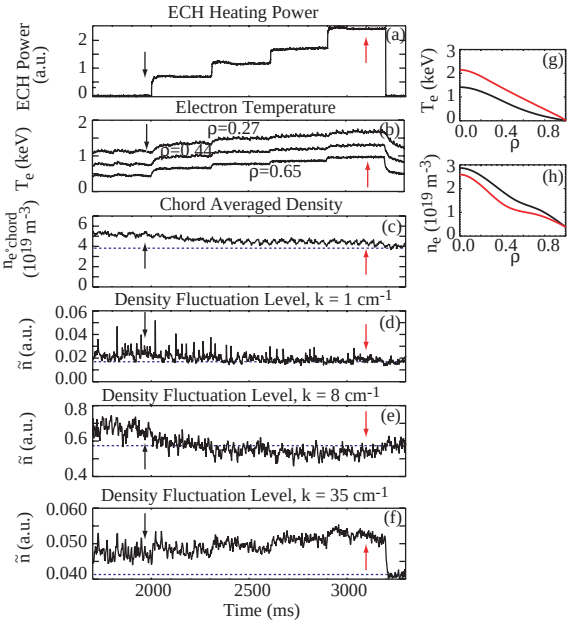

Fig. 8. Time series of (a) electron cyclotron heating, (b) electron temperature, (c) chord averaged density, (d) integrated fluctuation level for k=1 cm^{-1} from FIR scattering, (e) integrated fluctuation level for k = 8 cm^{-1} from FIR scattering, (f) integrated fluctuation level for k=35 cm^{-1} from mm-wave backscattering, (g) electron temperature profiles from two times shown by the arrows in (a), and (f) density profiles for same two times.

except near ρ = 0.6. This appears to be inconsistent with the experimental measurement of little change in fluctuations at this k with ECH [either Fig. 8(d) or Fig. 9(a)] however, preliminary calculations of the E×B shearing rate show it to be far above these growth rates except around ρ = 0.6. Such a large shearing rate could suppress the low-k fluctuations everywhere except near ρ = 0.6 where there is little change in the growth rates. Interestingly, the predicted real frequency is in the ion direction only near ρ = 0.6, being in the electron direction everywhere else. The growth rates for k = 8 cm^{-1} both decrease and increase depending upon the radial location [Fig. 9(e)]. While the total fluctuation signal from k = 8 cm^{-1} decreases [Fig. 8(e)], the k = 8 cm^{-1} frequency spectrum response varies with frequency, increasing for negative frequencies, and decreasing for positive frequencies [Fig. 9(b)]. Since the signal comes from different radii, the different frequencies may be associated with different radial positions, thus indicating a radial variation in the fluctuation response. Finally, the k = 35 cm^{-1} growth rates decrease everywhere except near the edge where an increase is observed [Fig. 9(f)]. The experimental data clearly shows an increase [Fig. 8(f) or Fig. 9(c)] which appears inconsistent with the signal coming from a radial extent of ρ = 0.4 to 1.0. It should be noted that earlier data from various conditions are consistent with the high-k signals originating from a radial location of ρ ≈ 0.8 and greater. Such a spatial distribution would bring the linear growth rate calculations into better agreement with the measurement. This is a very interesting observation with more work needed to fully understand it. One speculation is that interactions of the high-k fluctuations with lower k's might change the saturation level (e.g. see [6]).

6. Conclusions

In conclusion, density fluctuations measurements have been obtained on DIII-D over a very broad wavenumber range (k ≈ 1→35 cm^{-1} or $k_\perp \rho_s \approx 0.2 \rightarrow 10$). These measurements show fluctuation activity over this wavenumber range, a range relevant to ITG, TEM and ETG,

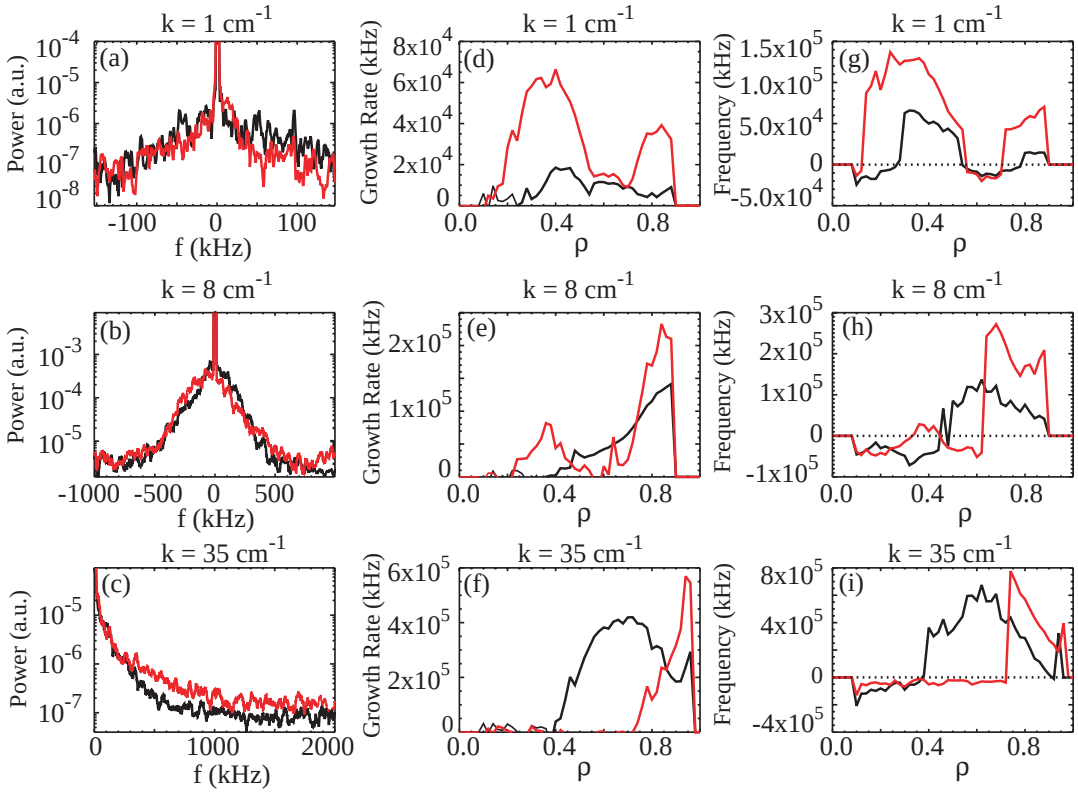

Fig. 9. Experimental power spectra versus frequency for the two times shown by arrows in Fig. 8 (black ohmic, red ECH). (a) k=1 cm^{-1} spectra from FIR scattering, (b) k=8 cm^{-1} spectra from FIR scattering, (c) k=35 cm^{-1} spectra from mm-wave backscattering. (d) through (i): GKS calculations for the same times and wavenumbers. Linear growth rates versus radial position: (d) k = 1 cm^{-1}, (e) k = 8 cm^{-1}, (f) k = 35 cm^{-1}. Real frequencies versus radial position: (g) k = 1 cm^{-1}, (h) k = 8 cm^{-1}, (i) k = 35 cm^{-1}.

which have qualitative agreement with linear gyrokinetic code calculations for the non-perturbed, Ohmic plasma case. Short duration neutral beam injection and ECH were used to modify the theoretical micro-instability growth rates as well as the experimentally measured fluctuation levels. The short duration NBI was found to be particularly effective in modifying only T_e. Experimentally, it was found that the fluctuations did not respond to the perturbations in the same manner across the wavenumber range, e.g. increasing at some k's and decreasing at others. The predicted linear growth rates also varied with wavenumber. Such variation confirms the need to concurrently measure a broad wavenumber range for comparison to simulations. Additionally, the predicted change in growth rates and measured variation in fluctuation signals for these perturbed plasma are in some cases inconsistent indicating the need for comparison to full non-linear simulations. These simulations are currently underway utilizing the GS2 [7] and GYRO [8] codes.

Acknowledgment

Work supported by U.S. Department of Energy under DE-FC02-04ER54698, DE-FG03-01ER54615, DE-AC02-76CH03073, SC-6832401 and DE-FG02-93ER54197.

References

[1] WALTZ, R.E., MILLER, R.L., Phys. Plasmas **6**, 4625 (1999).
[2] SLUSHER and SURKO, Phys. Fluids **23** 472 (1980).
[3] JENKO, *et al.*, Phys Plasmas **8** 4096 (2001).
[4] SINGH, *et al.*, Nucl. Fusion **41** 1219 (2001).
[5] DAVYDOVA, *et al.*, Phys Plasmas **9** 4623 (2002).
[6] HOLLAND, C. and DIAMOND, P., Phys. Plasmas **11** 1043 (2004).
[7] DORLAND, W., *et al.*, Phys. Rev. Lett. **85**, 5579 (2000).
[8] CANDY, J. and WALTZ, R.E., J. Comput. Phys. **186**, 545 (2003).